CERN–TH/99–394
MAN/HEP/99/6
MC-TH-99/18
December 1999

Diffractive production of high-p_t photons at HERA

B E Cox† and J R Forshaw‡§

† Department of Physics and Astronomy, University of Manchester, Manchester M13 9PL, UK

‡ Theory Division, CERN, 1211 Geneva 23, Switzerland

Abstract. We study the diffractive production of high p_t photons at HERA. We have implemented the process as a new hard sub-process in the HERWIG event generator in order to prepare the ground for a future measurement.

PACS numbers: 12.38Cy, 13.60.Fz, 13.85.-t

1. Introduction

One of the cleanest of all diffractive processes is that of diffractive photon production in the process $\gamma p \to \gamma Y$ where the photon carries a large p_t and is well separated in rapidity from the hadronic system Y. The process can be measured at HERA [1, 2, 3]. The largeness of the transferred momentum $-t \approx p_t^2 \gg \Lambda^2_{\rm QCD}$ ensures the applicability of perturbative QCD. Unlike diffractive meson production this process has the advantage that the hard subprocess is completely calculable in perturbation theory. The only non-perturbative component resides in the parton density functions of the proton that factorize in the usual manner.

Theoretical interest in this process dates back to the work of [4] where calculations were performed in fixed order perturbation theory and to lowest order in α_s. Recent work has extended this calculation to sum all leading logarithms in energy, for real incoming photons [2] and for real and virtual incoming photons [3]. The cross-section for $\gamma q \to \gamma q$ can be written

$$\frac{d\sigma_{\gamma q}}{dp_t^2} \approx \frac{1}{16\pi \hat{s}^2} \left|A_{++}\right|^2 \tag{1}$$

and we have ignored a small contribution that flips the helicity of the incoming photon. The photon-quark CM energy is given by $\hat{s}$. To leading logarithmic accuracy [2, 3]

$$A_{++} = i\alpha\alpha_s^2 \sum_q e_q^2 \frac{\pi}{6} \frac{\hat{s}}{p_t^2} \int_{-\infty}^{\infty} \frac{d\nu}{1+\nu^2} \frac{\nu^2}{(\nu^2+1/4)^2} \frac{\tanh \pi\nu}{\pi\nu} F(\nu)\ \mathrm{e}^{z\chi(\nu)} \tag{2}$$

§ On leave of absence from †.

where

$$z \equiv \frac{3\alpha_s}{\pi} \log \frac{\hat{s}}{p_t^2}, \tag{3}$$

$\chi(\nu) = 2(\Psi(1) - \mathrm{Re}\Psi(1/2 + i\nu))$ is the BFKL eigenfunction [5], $F(\nu) = 2(11 + 12\nu^2)$ for on-shell photons and there is a sum over the quark charges squared, e_q^2. The separation in rapidity between the struck parton and the final-state photon is $\Delta\eta \approx \log(\hat{s}/p_t^2)$.

The full photon-proton cross-section is obtained after multiplying by the parton density functions:

$$\frac{d\sigma}{dx dp_t^2} = \left[\frac{81}{16} g(x,\mu) + \Sigma(x,\mu)\right] \frac{d\sigma_{\gamma q}}{dp_t^2} \tag{4}$$

and we take the factorization scale $\mu = p_t$.

We have implemented this result in the HERWIG event generator in order to aid the experimental measurement of the process. We also note that having done this, it is a straightforward procedure to include the high-p_t production of vector mesons in a similar manner and we intend to do this in the near future. In this paper, we compare the HERWIG generated data with theory and discuss the strategy for a future measurement.

In order to speed up the event generation procedure, we used the following approximate parameterization:

$$\begin{aligned} G(z) \equiv & \int_{-\infty}^{\infty} \frac{d\nu}{1+\nu^2} \frac{\nu^2}{(\nu^2+1/4)^2} \frac{\tanh \pi\nu}{\pi\nu} 2(11+12\nu^2)\ \mathrm{e}^{z\chi(\nu)} \\ & \approx \frac{4.52}{(z+0.1)^{3/2}} \mathrm{e}^{4z\ln 2}\ \Theta(z-1) + (23.7 + 35 z^{2.3})\Theta(1-z) \end{aligned} \tag{5}$$

which is good to within a few percent over the z-range of interest.

2. Results

We show the p_t spectrum of the scattered photon in Figure 1. This plot is computed at fixed $W = 200$ GeV ($W^2 = \hat{s}/x$) and a fixed $\alpha_s = 0.2$. The choice to fix α_s is supported by Tevatron and HERA data on gaps between jets and high p_t diffractive vector meson production [6]. The solid curve shows the theoretical prediction derived directly from (4), it is compared to the HERWIG generated data at the parton level (before parton showers) and at the hadron level. We used the proton parton density functions of [7] (code 155 in PDFLIB [8]). The good agreement between theory and parton level is a check that the process is correctly implemented in HERWIG. The systematic shift arises because HERWIG ensures that energy and momentum are conserved and that final state hadrons are on shell [9].

In subsequent figures, we make the typical HERA cuts on the photon energy variable, $0.25 < y < 0.75$, and on the photon virtuality, $Q^2 < 0.01$ GeV^2. Statistical

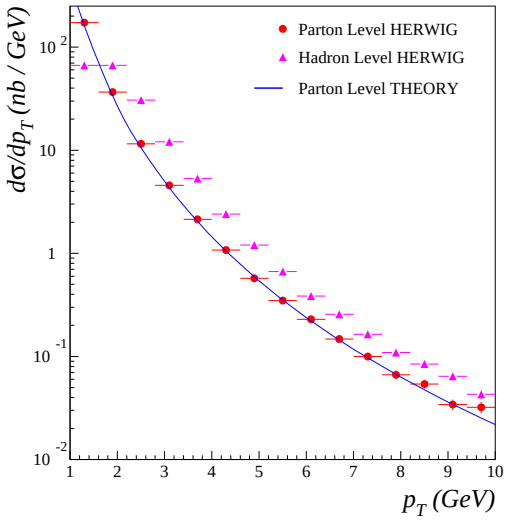

Figure 1.
The photon p_t spectrum.

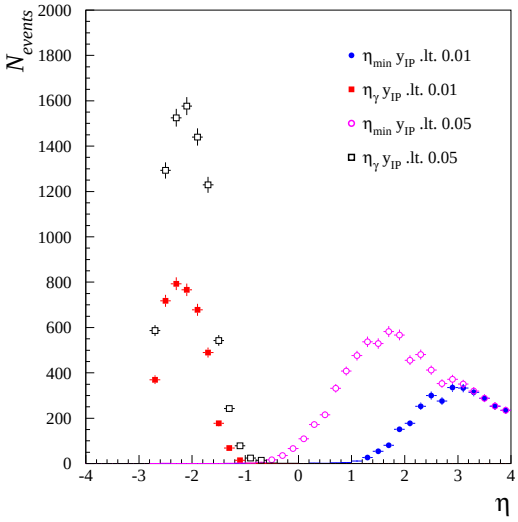

Figure 2.
The rapidities of the scattered photon and edge of system Y.

errors are shown corresponding to 44 pb^{-1} of ep data, typical of that already collected by each HERA experiment. We also make a cut $y_{I\!P} < 0.01$ where

$$y_{I\!P} = \sum_i \frac{(E - p_z)_i}{2E_\gamma} \approx \frac{p_t^2}{xW^2} \approx \mathrm{e}^{-\Delta\eta} \tag{6}$$

and the sum is over all final state particles excluding the electron and photon. Note that $y_{I\!P}$ can be measured accurately without needing to see the whole of system Y since the material lost at low angles does not contribute much to the numerator. As the last approximate equality shows, this cut ensures that the rapidity gap between the outoing struck parton and the outoing photon is bigger than about 4.5 units (recall that a large rapidity gap is a signal of diffractive processes). We have also integrated over all photon $p_t > 2.5$ GeV (and used $p_{\mathrm{tmin}} = 1$ GeV in the event generation).

The effect of varying the $y_{I\!P}$ cut on the size of rapidity gap can be seen in Figure 2, where we plot the rapidity of the scattered photon and the edge of system Y. By not requiring to measure system Y in detail it is possible to reach very high rapidity gaps. As the plot shows, gaps of 6 to 7 units in rapidity are not uncommon. Note that the limited y-range combined with the steeply falling p_t spectrum constrain the rapidity of the photon to be around $\eta \approx -2$.

In Figure 3 we show the $x_{I\!P}$ distribution and in Figure 4 the p_t distribution:

$$x_{I\!P} = \frac{(E + p_z)_\gamma}{2E_p} \approx \frac{p_t^2}{W^2}. \tag{7}$$

This variable can be measured to high accuracy. The steep rise at small $x_{I\!P}$ is driven by the BFKL kernel $\chi(\nu)$ in (2). In particular, the dominant conribution comes from

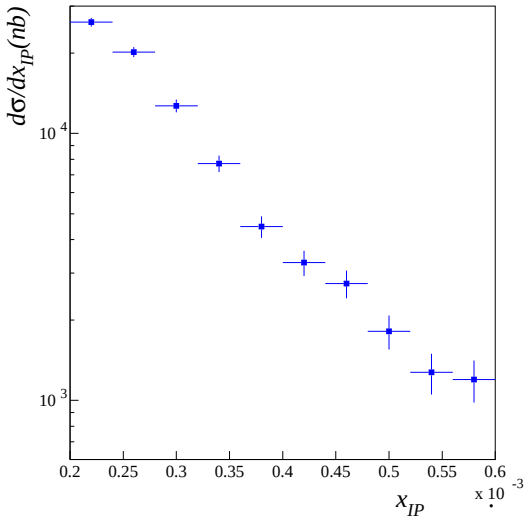

Figure 3.
The $x_{I\!P}$ distribution.

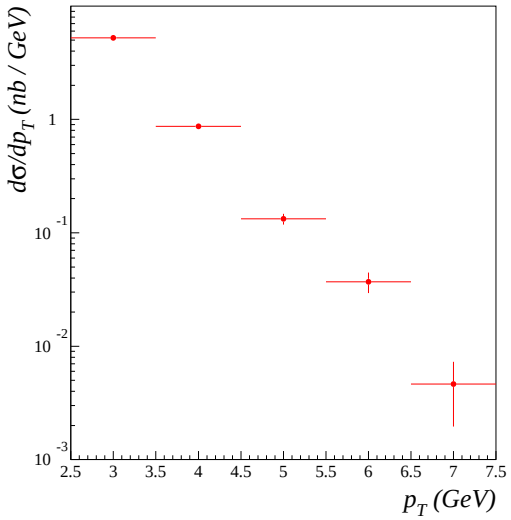

Figure 4.
The p_t distribution.

$\nu \approx 0$, and this leads to

$$\frac{d\sigma}{dx_{I\!P}} \sim \frac{W^2}{p_t^4} \mathrm{e}^{2z\chi(0)} \sim \frac{1}{W^2} \left(\frac{1}{x_{I\!P}}\right)^{2\omega_0+2} \tag{8}$$

where $\omega_0 = (3\alpha_s/\pi)4\ln 2$ in the LLA. It will be interesting to see to what degree the measured $x_{I\!P}$ distribution follows this power-like behaviour.

Acknowledgments

We thank Jon Butterworth and Norman Evanson for their help.

References

[1] Ginzburg I F and Ivanov D Yu 1996 *Phys. Rev.* **D54** 5523
[2] Ivanov D Yu and Wüsthoff M 1999 *Eur. J. Phys.* **C8** 107
[3] Evanson N G and Forshaw J R 1999 *Phys. Rev.* **D60** 034016
[4] Ginzburg I F, Panfil S L and Serbo V G 1987 *Nucl. Phys.* **B284** 685
[5] Balistky I and Lipatov L N 1978 *Sov. J. Nucl. Phys.* **28** 822
[6] Cox B E, Forshaw J R and Lönnblad L 1999 *JHEP* **10** 023
Forshaw J R, 1999 *Nucl. Phys.* (Proc. Suppl.) **79** 311
[7] Glück M, Reya E and Vogt A 1995 *Z. Phys.* **C67** 433
[8] Plothow-Besch H, W5051 PDFLIB, 1997.07.02, CERN-PPE
[9] Cox B E and Forshaw J R 1998 *Phys. Lett.* **B434** 133